Sadeghi Susan (Orcid ID: 0000-0003-2917-4920)

A sensitive fluorescent probe based on dithizone-capped ZnS quantum dots for quercetin determination in biological samples

Susan Sadeghi[*,a], Mohadeseh Hosseinpour-Zaryabi[a]

[a] Department of Chemistry, Faculty of Science, University of Birjand, P.O. Box. 97175/615, Birjand, Iran

Abstract

A simple turn on/off fluorescence approach based on the dithizone-capped ZnS quantum dots (ZnS@DZ QDs) with the help of lead ions as a fluorescent probe for the quantitative determination of quercetin is reported. The interaction of lead ions with dithizone led to form a rigid structure on the surface of ZnS@DZ QDs and turned on the fluorescence intensity of the QDs. After addition of quercetin to this probe and interaction with lead ions, the fluorescence emission turned off. Concerning the quenching fluorescence intensity of ZnS@DZ QDs/Pb^{2+} QDs probe induced by the target, under the optimal conditions, the probe enables to detect quercetin in the concentration range from 0.54 μM to 21.7 μM with a correlation coefficient of 0.993 and detection limit of 0.25 μM. The present probe was applied successfully to the determine quercetin as a nutritional biomarker in human serum and 24-h urine samples.

Keywords: Quercetin; Dithizone-capped ZnS quantum dots; Fluorescence; Lead ion

* Corresponding author. Tel/Fax: +98 5632202009
E-mail address: ssadeghi@birjand.ac.ir (S. Sadeghi)

This article has been accepted for publication and undergone full peer review but has not been through the copyediting, typesetting, pagination and proofreading process which may lead to differences between this version and the Version of Record. Please cite this article as doi: 10.1002/bio.3903

1. INTRODUCTION

A biomarker is considered as an indicator of a pathogenic process, a normal biologic process, or a pharmacological response to a therapeutic disorder.[1] Nutritional biomarkers are biological compounds that provide clinical information regarding the intake or metabolites of foods. [1] The intake of nutritional biomarkers by consumption of fruits and vegetables has been given special attention to the evaluation of health food diet.[2-4] It is found that polyphenols have potentially beneficial effects on health, so that there is a close relationship between cancer and specific polyphenol-rich food consumption. Specific polyphenols can be considered as a nutritional biomarker and provides valuable information about total polyphenol intake. One group of the polyphenolic compounds with anti-viral, anti-hepatotoxic, therapeutic, and anti-bacterial properties that can be considered in human diets is flavonoids.[5-8] To evaluate the efficacy of significant flavonoids in the human food and its usefulness as a biomarker in vegetable and fruit groups, it is necessary to control the concentration of flavonoids in the diet along with human biological samples. It is well known that the nature of polyphenols and source of the food, the dose and time significantly affect the concentration of these compounds in plasma. However, 24-h urinary excretion of total phenols can be considered as a biomarker of the intake from fruit and vegetables and accumulation of these compounds in the human body. One of the polyphenols exerts in urine that also can be considered as a biomarker of total polyphenol intake is quercetin.[9] Quercetin, 3, 3', 4', 5', 7-pentahydroxy flavone, as a subclass of flavonoides, is a beneficial flavonoid with anti-contraction, antioxidant and anti-tumor activity to treat some cancers, and diabetes.[10-12] It was found that quercetin, in combination with other flavonoids, might reduce the lung cancer risk.[13] Despite high amount of quercetin obtained from foods, due to its poor solubility in water and instability in biological fluids, only less than seven percents of the amount of quercetin consumed is detected in urine samples.[12, 14] Therefore, there is need to

perform an appropriate sensitive and robust method to determine low concentration of quercetin in complex matrices such as serum and urine fluids. High performance liquid chromatography (HPLC) and liquid chromatography-mass spectrometry often used for the determination of quercetin.[15] However, these techniques are expensive, time consuming and require the use of toxic solvents. Other analytical methods such as capillary electrophoresis,[16, 17] UV-Vis and Raman spectroscopy,[18, 19] and electrochemical techniques[20] have also been used to determine quercetin. Although spectrophotometric methods for the determination of quercetin like Folin–Ciocalteu assay are relatively inexpensive, but they are non-specific methods.[21, 22] Therefore, fast, sensitive, and inexpensive but reliable methods for the determination of quercetin are demanded. Recently, determination of quercetin was carried out by fluorometry using semiconducting quantum dots.[23,24] The distinctive properties of quantum dots include high brightness, broad absorption and narrow emission spectra in peak width, continuous but controllable emission and long term stability compared to conventional organic fluorescent dyes favored them in fluorescence chemical analysis. Besides, semiconducting quantum dots have high resistance to photobleaching, so that they can be applied as optical sensing probes.[25]

Interaction between the surface atoms of a fluorophore and the surrounding molecules may be remarkable influences on the fluorescence intensity. Semiconductor nanoparticles as useful fluorescent probes can be used for the analysis of biological and pharmaceutical compounds over the past decade. To improve the sensitivity of these nanoparticles, modification of their surfaces with appropriate receptors enables them to interact selectively with the target. ZnS quantum dots (Zns QDs) as a direct bandgap semiconductor have chemical stability against oxidation and hydrolysis. ZnS QDs show unique properties because of quantum confinement effects that make it as promising materials for sensor and biosensor applications. [26, 27] ZnS QDs have been used as a label free probe for sensitive detection of

biological species. [28] Also, it has an efficiency of antibacterial, antifungal, and antioxidant properties through generation of electron or redox reaction. Capping of ZnS QDs with an appropriate functional material provides great potential of QDs in the field of biological and environmental analysis. Recently, metal ion replacement has been employed in fluorescent probes for turn-off detection of small molecules or ions. [29] This approach seems to enhance the selectivity of the probe to the target.

Dithizone (DZ) as a classic chelating agent is capable of coordinating with metal ions via amine or thiol groups whose complexes have high sensitivity, and stability. The objective of this study was to develop of a simple, rapid, sensitive and selective optical method for the quantitative determination of quercetin in aqueous samples. This method is based on using ZnS QDs capped with dithizone (ZnS@DZ QDs) by with the assistance of Pb^{2+} ions as a chemical nanosensor. Upon exposure ZnS@DZ QDs to pb^{2+} ions, its interaction with DZ at the surface of ZnS QDs inducing a fluorescence emission enhancement. By adding quercetin to this system, because of high affinity of quercetin toward pb^{2+} ions, a ternary interaction among Pb^{2+}, ZnS @DZ and quercetin is occurred. In this way, displacement of Pb^{2+} from the ZnS@DZ QDs surface toward quercetin decreases the fluorescence intensity gradually. Based on this approach, a combination of amplification and quenching of fluorescence intensity of this probe provides a new strategy for sensing of quercetin with high sensitivity. Notably, the response time of the probe is fast, candidating it for real time analysis.

2. EXPERIMENTAL

2.1 Materials

Quercetin was provided by Sigma-Aldrich Corporation (Darmstadt, Germany). Isoleucine, cysteine, valine, methionine, uric acid, urea, glutamic acid, arginine, glucose and ascorbic acid were provided from Merck (Darmstadt, Germany) with analytical grade and used

without further purification. The nitrate salts of cations and sodium salts of anions were purchased from Merck. The water used in all experiments was deionized and provided by an Aqua Max 370 water purification system (Young-Lin, Korea).

2.2 Apparatus

Fluorescence spectra were recorded on a Shimadzu RF-5301PC spectrofluorometer (Shimadzu, Japan) equipped with a 10 mm path-length quartz cell and the excitation and emission bandwidths adjusted to 5 nm. UV 2501PC-spectrophotometer (Shimadzu, Japan) with a 1.0 cm optical path length quartz cell was used to recording the UV–visible spectra. A Benchtop pH meter model BP3001 was utilized to adjust the pH values of the aqueous solutions (Trans Instrument, Singapore). The X-ray diffraction (XRD) pattern of ZnS@DZ QDs was recorded in the range 2θ = 20-80° on a PHILIPS-PW1730 diffractometer using a monochromatic X-ray beam with Cu K_α radiation. Fourier transform infrared spectra (FT-IR) of each sample were recorded in the 500-4000 cm^{-1} wavenumber range with Perkin Elmer Spectrum Two FT-IR spectrometer (Liantrisant, UK). The morphological feature of the sample was characterized by transmission electron microscopy (TEM, Zeiss-model EM10C, Germany) operating at 100 KV. The dilute aqueous solution of sample was sonicated for 15 min by Misonix sonicator (Misonix- S3000, USA) and then one drop of the sample was dropped onto a formvar carbon film on copper grid 300 mesh (EMS, USA) and dried thoroughly at room temperature.

2.3 Synthesis of ZnS@DZ QDs

The ZnS nanoparticles were synthesized by a hydrothermal method according to the previous report.[30] Briefly, 25 ml of the equimolar aqueous solution of zinc acetate and thioacetamide (0.5 M) were mixed followed by sonication for 10 min. Then, the mixture was heated to 85°C for 3 hours. The white precipitate was washed three times with water and ethanol and dried at 60 °C for 12 hours.

Dithizone functionalized zinc sulfide quantum dots (ZnS@DZ QDs) were synthesized by dispersing 10 mmol of ZnS nanoparticles and 10 mmol of dithizone in 10 mL ethanol under vigorous stirring for 1 hour at room temperature. The final pink powder was separated by centrifuging at 5000 rpm, washed with water several times and dried at 60 °C for 12 hours.

2.4 Analytical procedure

For fluorescence intensity measurement, ZnS@DZ QDs solution (38.9 μg mL^{-1}) and Pb^{2+} ion (29.0 μg mL^{-1}) were mixed thoroughly in a sample tube and diluted to 5 mL with phosphate buffer (pH 2.6, 0.1 M). Aliquot of quercetin solution (50 μL) in a concentration range of 0.5-75 μM was then added to the sample tube and mixed completely. The fluorescence intensity of the mixture was measured immediately. The fluorescence spectra were recorded using an excitation and emission wavelengths set at 280 and 364 nm, respectively. Changes in fluorescence intensity as $\Delta F = F_0 - F$, where F and F_0 are the fluorescence intensities of the solution containing ZnS@DZ QDs and Pb^{2+} ions with and without quercetin, respectively, were used as an analytical response to construct the calibration curve.

2.5 Preparation of real samples

The urine (U1-U6) and serum (S1-S6) samples were obtained from healthy persons aged 30-65 years. The urine samples were filtered and diluted for 20 times before analysis. To prepare the serum samples, an appropriate amount of sodium chloride was added to 0.5 mL of human serum so that the final concentration of sodium chloride was 0.1 M, and incubated for 60 min.[31] Then, the equivalent volume of methanol was added to the above mixture and incubated for further 60 min. The resulting precipitate was separated by centrifuging at 4000 rpm. To remove methanol, the supernatant was dried using a gentle stream of nitrogen gas. The residue was diluted to 10 mL. The urine and serum samples were treated according to the procedure described in the assay section.

3. RESULTS AND DISCUSSION

3.1 Characterization of the ZnS@DZ QDs

The FT-IR spectra of the synthesized ZnS QDs and ZnS@DZ QDs are given in Fig. 1. The broad absorption band of O-H stretching vibration of adsorbed H_2O on the surface of the quantum dots is located at 3200 cm^{-1} (Fig. 1A-a). The two peaks situated around 1037 cm^{-1} and 678 cm^{-1} are corresponded to the S-O and Zn-S stretching vibrations, respectively.[30] The two absorption bands at 1560 and 1428 cm^{-1} can be ascribed to the asymmetrical and symmetrical C=O stretching vibrations, respectively. These peaks observed in ZnS QDs FTIR spectrum, whilst they disappeared in the spectrum of ZnS@DZ QDs likely due to leaving the carboxylate from ZnS QDs surface and capping with dithizone (Fig. 1A-b). Additionally, two absorption bands located at 1025 cm^{-1} and 1116 cm^{-1} attributed to –N=N– and C-S vibration frequencies indicating that capping of ZnS QDs was occurred by dithizone. The optical UV-Vis absorption spectrum of freshly prepared ZnS QDs dispersed in aqueous solution is shown in Fig. 1B. It exhibited a maximum absorption peak at 260 nm with a blue-shifted from the band gap wavelength of bulk ZnS (λ_{max} = 340 nm). According to the literature, an absorption peak occurring between 225 and 260 nm has been associated with the formation of nanosized ZnS. DZ as a ligand posses high affinity to metal ions and enable to form complex with Zn^{2+} in enolic form in ethanol medium.[32] Immobilization of DZ on the surface of the ZnS QDs may occur via a surface coordination with Zn^{2+} ions to form DZ- Zn complex. The evidence for such changes is appearance a definite pink hue solid. This event was supported by investigation of the optical absorption spectra of DZ, ZnS QDs, and ZnS@DZ QDs dispersed in aqueous solutions. The ethanolic solution of dithizone exhibits two absorption bands with maxima at 450 and 610 nm due to the thione and thiol tautomers, respectively (Fig. 1B). In addition, an absorption spectrum for the ethanolic solution of Zn^{2+}-dithizonate complex (DZ-Zn^{2+}) exhibits a maximum at 520 nm which is located close to the

minimum in the absorption spectrum for dithizone (Fig. 1B). A small shoulder was seen at wavelengths longer than 590 nm that was attributed to residual and unreacted dithizone in this phase. The first excitonic absorption peak of ZnS@DZ QDs centered at 520 nm demonstrating the DZ-Zn^{2+} complex formation on the surface of ZnS QDs.

The fluorescence spectrum of ZnS QDs presents the maximum emission wavelength at 364 nm upon excitation at 280 nm (Fig. 1C).

The photoluminescence intensity of ZnS QDs at 364 nm is increased upon addition of DZ with no remarkable changes in the peak position or band shape because of no effective spectral overlapping of ZnS@DZ QDs absorption and emission spectra (Fig. 1D). This attributed to the formation of ZnS-DZ and interaction DZ with Zn^{2+} at the surface of QDs.

The crystalline structure of the prepared ZnS QDs was characterized using X-ray diffraction (XRD) pattern which is illustrated in Fig. 1E. The wide angle XRD pattern of ZnS nanocrystals corresponded to a cubic blended crystal structure of ZnS with peaks for crystal planes (111), (220) and (311) observed at 2θ values of 29.2°, 48.4° and 57.0°, indicating formation of pure ZnS nanocrystals.[30] The diameter of the ZnS crystallite particles by the Debye-Scherrer equation was estimated to be about 3.6 nm.

Fig. 1F shows a typical TEM overview image of ZnS QDs. The TEM image indicates the ZnS nanocrystals as roughly spherical, ranging from 3 to 10 nm with the average diameter of 5 nm.

The nanoparticle size of ZnS@DZ QDs was also evaluated by the effective mass approximation Brus model using the band gap energy.[33] The band gap energy for a direct transition was estimated through absorption spectrum by drawing $(\varepsilon h\nu)^2$ versus $h\nu$ by Tauc equation where hν is the photon energy of the incident light, and ε is the absorption coefficient.[34] The value of optical band gap was obtained from the first excitonic absorption

peak of the UV–Vis spectrum of ZnS@DZ QDs. The evaluated band gap energy was 5.0 eV which was higher than the value of bulk ZnS (3.68 eV), confirming that the particles size was smaller than the bulk ZnS due to the quantum confinement. The particle size of the ZnS@DZ nanocrystals was estimated 3.2 nm which is verified by the XRD result.

3.2 Effect of metal ion on photoluminescence enhancement

In preliminary experiments, to evaluate the affinity of ZnS@DZ QDs to some metal ions, the fluorescence intensity of the ZnS@DZ QDs in the absence and presence of some alkaline and transition metals including Cu^{2+}, Ca^{2+}, Pb^{2+}, Zn^{2+}, Mn^{2+}, Co^{2+}, Ni^{2+}, Cd^{2+}, Fe^{3+} and Cr^{3+} (100 µM) was investigated. The plot of the differences in the ZnS@DZ QDs fluorescence intensities in the presence and absence of metal ion, as a response,versus various metal cations are illustrated in Fig. 2. Among the treated metal ions, the fluorescence of DZ-functionalized ZnS QDs was turned on upon addition of Pb^{2+}, while other cations did not enhance the fluorescence intensity. After addition of quercetin to the functionalized ZnS QDs with dithizone in the presence pb^{2+} ions, the fluorescence intensity was strongly quenched without being accompanied by a shift in the maximum emission peak position (Fig. 1D). The responses as $F-F_0$, where F and F_0 are the fluorescence intensities of the solutions containing ZnS@DZ QDs and metal ion with and without quercetin, respectively, are shown in Fig. 2. Quercetin interaction with this system induced a fluorescence quenching. Quercetin possesses three possible chelating sites: the 3-hydroxy-carbonyl, the 5-hydroxy-carbonyl, the catechol group (3′,4′-dihydroxyl) in ring B and and the 3-hydroxy-carbonyl, the 5-hydroxy-carbonyl in rings C and A, respectively. [35] The catechol moiety is the most reactive site to deprotonate easily and coordinate with Pb^{2+}. Because, various factors rather than the analyte can induce the direct quenching of a probe, the turn on/off mode for fluorescence detection of target

analyte is challenging. Therefore, the ZnS@DZ QDs in the presence of Pb^{2+} ions can be a good candidate as a sensitive fluorescent probe for quercetin measurement.

3.3 Optimization of significant variables

The analyte to probe binding were significantly affected by different key variables such as sample pH, probe concentration, and incubation time which were optimized in a one variable at a time approach.

3.3.1 Effects of pH and buffer

The behavior of the ZnS@DZ QDs/Pb^{2+} probe toward quercetin in phosphate buffer at different pH values within the range 2-10 was investigated. The results showed that the response raised up to pH 2.6 and gradually reduced to pH 6 and after that it remained constant until pH 8 (Fig. 3). In acidic solution, DZ binds in the keto form to zinc ions on the surface of ZnS QDs, so that the sulfur atom in the DZ structure can bind to the lead ions and the fluorescence intensity of ZnS QDs increased (Fig. 3B). The decrease in the response of the probe at pH > 3 is prpbably due to the instability of keto form of dithizonate. Also, the pH effect on the emission ZnS@DZ QDs in the absence of pb^{2+} toward quercetin was examined and showed that the response of the ZnS@DZ QDs didn't significant change in the pH range from 2 to 8, confirming that the quercetin could interact with DZ on the surface of ZnS@DZ QDs. Even in strong alkaline environments, the lead dithizonate is stable and the response didn't change.

In order to investigate the influences of buffer on fluorescence intensity of the probe, three buffers (citrate, phthalate and phosphate) at pH 2.6 were selected. The results revealed that the probe in phosphate buffer had the highest sensitivity to quercetin. Additionally, five solutions at different phosphate buffer concentrations ranged from 0.01 to 0.1 M at pH 2.6 were prepared and the responses of the probe upon addition of quercetin were examined. The

increase in buffer concentration resulted in an increase in the probe response, so that 0.1 M phosphate buffer was used for further studies.

3.3.2 Effect of Pb^{2+} concentration

The fluorescence spectra of ZnS@DZ in determination of quercetin were recorded in the absence and presence of Pb^{2+} ions. In this study, first Pb^{2+} ions were added to the solution containing ZnS@DZ QDs and allowed to react for 2 min before the addition of quercetin. The changes in fluorescence intensity with lead ion concentrations over the range 4.8-140 µM at pH 2.6 are shown in Fig. 4. Differences in fluorescence intensities of the ZnS@DZ QDs for quercetin determination at 364 nm in the presence and absence of Pb^{2+} were plotted against different concentrations of Pb^{2+} ions. As illustrated in the inset of Fig. 4, the response is increased along with the increase of Pb^{2+} concentration, indicating that Pb^{2+} plays an imprtant role in the interaction of ZnS@DZ QDs with quercetin. However, due to the limitation in reading the luminescence intensity beyond 1000, the concentration of lead ions was selected at 140 µM (29.0 µg mL^{-1}).

3.3.3 Effect of concentration of ZnS@DZ QDs

The quantum dots concentration not only affects the luminescence intensity, but also the sensitivity of the measurement. The concentrations of ZnS@DZ QDs within the range from 3.0 to 52 µg mL^{-1} were employed. As the results are illustrated in Fig. 5, the ΔF gradually increased up to 36 µg mL^{-1} and was constant within the concentration range of 36–40 µg mL^{-1} and after that it decreased, so that 39 µg $mL^{-1}$of the ZnS@DZ QDs was chosen for further studies.

3.3.4 Effect of Reaction time

Response time of the probe toward quercetin was also investigated. The results revealed that the interaction between quercetin and the probe occurred rapidly at room temperature and the fluorescence intensity remained constant for 60 min.

3.4 Analytical features

The fluorescence spectrum of the developed probe with quercetin exposure at various concentrations is illustrated in Fig. 6A. The calibration plot of the ΔF response against quercetin concentrations(C_{Que}) is depicted in Fig. 6B. The linear fitting of the plot was obtained in the range of 0.54 to 21.7 µM with the equation $\Delta F = 32.48\ C_{Que} + 36.6$ and the correlation coefficient of 0.9930 (inset of Fig. 6B). The limit of detection was evaluated using three standard deviation of the blank signal divided by the slope of the calibration plot and found to be 0.25 µM. The precision of the method as the relative standard deviation (RSD %) for 8 replicate measurements of quercetin at 1.1 µM concentration level was 2.1%.

3.5 Quenching mechanism

According to the FT-IR spectra, DZ in enolic form interacts with the surface of ZnS QDs via amine and thiol groups to accommodate its complex with pb^{2+} ions on the surface of QDs. As a consequence, this chelation enhances fluorescence intensity of ZnS QDs. The absorption spectrum of Pb^{2+}-DZ complex in aqueous solution unchanged in the absorption spectrum of ZnS@DZ QDs dispersed in aqueous solution, indicating no inner filter resulted from the absorption of the Zn@DZ QDs/Pb^{2+} (Fig. 7).The fluorescence intensity of ZnS@DZ QDs is also effectively enhanced after interaction with Pb^{2+} (turn on) with no blue or red shift in the photoluminescence profile (Fig. 1 D), implying that a complex formation between DZ and Pb^{2+} occurred on the surface of ZnS@DZ QDs. Hence, probably conformational rigidity of the ZnS@DZ QDs/Pb^{2+} enhanced the fluorescence intensity. Pb^{2+} ions also enable to coordinate with quercetin (log β_2 = 7.71) via catechol site.[36-38] Before and after quercetin addition, the fluorescence excitation and emission wavelengths of Zn@DZ QDs were almost unchanging (Fig. 1D), which indicated to static quenching mechanism upon formation of the ground-state complex. [37] Addition of quercetin to the probe didn't appear new absorption band in the absorption spectrum of Zn@DZ/Pb^{2+} probe, confirming no direct bonding

between quercetin with the Zn@DZ QDs (Fig. 7). It seems the competition of dithizone and quercetin for pb^{2+} coordination has probably led to partially moving the pb^{2+} ions away from the surface of QDs after the addition of quercetin. This event may reduce the rigidity of the DZ/Pb^{2+} complex on the surface of ZnS@DZ QDs and immideately fluorescence emission decreases (turn off). Meanwhile, the hydroxyl and carboxyl groups of quercetin have an electron withdrawing property, so that they can be considered as an excellent electron acceptor. Hence, electron transfer from the excited QDs to the Pb^{2+}-quercetin complex may also involve in the proposed quenching mechanism. The probable mechanism for the detection of quercetin is presented in Scheme 1.

A Stern-Volmer analysis of the emission quenching of the probe was carried out according to the linear relationship between F_0/F and quercetin concentration ([Que]) as the following (Eq. 2):

$$\frac{F0}{F} = 1 + K_{SV} . [Que] \quad (2)$$

where F_0 and F are the fluorescence intensities of the $ZnS@DZ/Pb^{2+}$ probe in the absence and presence of the quercetin, respectively, K_{SV} and [Que] are referred to the Stern-Volmer quenching constant and the concentration of quercetin (μM), respectively (Fig. 6C). The obtained K_{SV} of 1.045×10^5 L mol^{-1}, suggesting quercetin has a quenching effect for the fluorescent probe.

3.6 Effect of co-existing substances

To evaluate the selectivity of probe to quercetin, the effect of ions and substances commonly found in urine and serum on the response of the probe was studied. Several experiments were designed for binary solutions containing analyte and possible interferents and analyzed according to the developed method. The tolerance limit of an interferent is defined as the concentration of a substance that showed more than ± 10% influences on the fluorescence intensity of the $ZnS@DZ\ QDs/Pb^{2+}$ probe (Table 1). The results indicated that

most of the investigated coexisting substances didn't have a significant effect on fluorescence intensity up to 1000 fold excess than the analyte concentration, implying that the probe was high selective to quercetin and making it suitable for the fast and accurate detection of quercetin in real samples.

3.7 Application

The concentrations of quercetin in human serum and urine 24h samples were determined by the developed method. Human serum and urine 24h samples were treated nased on the developed analytical procedure and standard addition method was used for quantitative analysis. As shown in Table 2, the recoveries are in the range of 90-110% with the relative standard deviations (RSD%) for three measurements ranged from 0.8% to 13.2% and 0.3% to 19.5% for urine and serum samples, respectively. These results suggest that the proposed sensing system can rapidly detect endogenous quercetin in human serum and urine samples.

3.8 Comparison of the proposed method with the other reported methods for detection of quercetin

The analytical features of the developed method have been compared with other reported fluorescene methods.[19, 23, 24, 37, 39-41] The results in Table 3 indicates that the linear range of the developed method is wider than phosphorescence and fluorescence methods with MPA-ZnS QDs.[23, 37] In addition, the developed method is more sensitive with lower detection limit if compared with Raman spectroscopy,[19] fluorescence method using CdSe/ZnS quantum dots,[24] spectrophotometric method[39] and flow injection chemiluminescence detection.[40] However, it is less sensitive to quercetin than photoluminescence methods using carbon nanoparticles.[41] This method is suitable for biological fluids and suffers from less background interference.

4. CONCLUSIONS

A new methodology has been developed for sensing of quercetin based on the monitoring quenching of fluorescence signal of the nanosensor ZnS@DZ QDs/Pb^{2+}. The ligand-binding affinity with Pb^{2+} metal ions during the recognition and the nature of the complex formation under the specific sensing conditions, provided a selective method for the determination of quercetin. The difference in fluorescence intensity of the probe with and without quercetin was used as a analytical response. The fast quenching of fluorescence intensity of the probe correlated in a linear manner with the analyte concentrations. The developed fluorescence assay indicated a high degree of sensitivity to the quercetin with a detection limit of 0.25 µM. The performance of the probe did not significantly change with the matrix of serum and urine samples. The response time of the developed sensor is fast, making it for the instant quercetin monitoring application.

ACKNOWLEDGEMENTS

This work was supported in part by the Birjand University Research Council (Grant No. 1396D12158) and gratefully acknowledged.

Compliance with ethical standards

Conflict of interest

The authors declare that they have no conflict of interest.

Susan Sadeghi ORCID iD https://orcid.org/0000-0003-2917-4920

REFERENCES

[1] K. Strimbu and J. A. Tavel, Current Opinion in HIV and AIDS, 2010, 5, 463-466.

[2] J. H. M. De Vries, P. C. H. Hollman, S. Meyboom, M. N. C. P. Buysman, P. L. Zock, W. A. Van Staveren and M. B. Katan, Am. J. Clin. Nutr., 1998, 68, 60-65.

[3] J. V. Woodside, J. Draper, A. Lloyd and M. C. McKinley, Proc. Nutr. Soc., 2017, 76, 308-315.

[4] M. Russo, C. Spagnuolo, I. Tedesco, S. Bilotto,and G. L. Russo, Biochem. Pharmacol. 2012, **83**, 6–15

[5] Z. Chen, S. Qian, J. Chen and X. Chen, J. Nanoparticle Res., 2012, 14, 1264-1272.

[6] A. Medina-Remón, A. Tresserra-Rimbau, S. Arranz, R. Estruch and R. M. Lamuela-Raventos, Bioanalysis, 2012, 4, 2705-2713.

[7] S. E. Nielsen, R. Freese, P. Kleemola and M. Mutanen, Cancer Epidemiol. Biomark. Prev., 2002, 11, 459-466.

[8] R. Q. Aucelio, J. M. Carvalho, J. T. Real, L. Maqueira-Espinosa, A. Pérez-Gramatges and A. R. da Silva, Spectrochim. Acta A, 2017, **172**, 147-155.

[9] A. Day and G. Williamson, Br. J. Nutr., 2001, 86, S105-S110.

[10] Z. Zhang, Y. Miao, L. Lian and G. Yan, Anal. Biochem, 2015, 489, 17-24.

[11] P. Iranmanesh, S. Saeednia, M. Nourzpoor, Chinese Phys B 2015, 24, 046104

[12] Y. Liu and M. Guo, Molecules, 2015, **20**, 8583-8594.

[13] L. Le Marchand, S. P. Murphy, J. H. Hankin, L. R. Wilkens and L. N. Kolonel, J. Natl. Cancer Inst. Monogr., 2000, 92, 154-160.

[14] K. Dwiecki, P. Kwiatkowska, A. Siger, H. Staniek, M. Nogala-Kałucka and K. Polewski, J. Food Sci. Technol., 2015, 50, 1366-1373.

[15] V. Pilařová, K. Plachká, L. Chrenková, I. Najmanová, P. Mladěnka, F. Švec, O. Novák and L. Nováková, Talanta, 2018, 185, 71-79.

[16] S. Verónica C, F. María De Los Ángeles, G. Claudio R and S. M. Fernanda, Anal. Methods, 2014, 6, 4878-4884.

[17] S. Şanli and C. Lunte, Anal. Methods, 2014, 6, 3858-3864.

[18] H. F.Askal, G. A. Saleh, and E. Y. Backheet , Talanta 1992, 39, 259-63.

[19] Y. Numata and H. Tanaka, Food Chem, 2011, 126, 751-755.

[20] D. Zielińska, L. Nagels and M. K. Piskuła, Anal. Chim. Acta, 2008, 617, 22-31.

[21] H. Ali Mahmood and S. S. Abed, Asian J. Chem., 2018, 30, 1691-1695.

[22] P. Matić, M. Sabljić and L. Jakobek, J. AOAC Int., 2017, 100, 1795-1803.

[23] D. Wu and Z. Chen, Luminescence, 2014, 29, 307-313.

[24] W. P. Hu, G. D. Cao, W. Dong, H. B. Shen, X. H. Liu and L. S. Li, Anal. Methods, 2014, 6, 1442-1447.

[25] E. Safitri, L. Y. Heng, M. Ahmad, T. L. Ling, Sensors Actuat. B-Chem, 2017, 240, 763-769.

[26] Y. Xiong, M. Liang, Y. Cheng, J.i Zou and Y. Li, Analyst, 2019, 144, 161-171.

[27] S. A. Nsibande, P. B.C. Forbes, Luminescence. 2019, 34, 480-488.

[28] I. V. Martynenko, D. Kusic, F. Weigert, S. Stafford, F.C. Donnelly, R. Evstigneev, Y. Gromova, A. V. Baranov, B. Rühle, H.-J. Kunte, Y. K. Gun'ko, U. Resch-Genger, Anal. Chem., Anal. Chem. 2019, 91, 12661–12669.

[29] E. M. Nolan, and S. J. Lippard, Chem Rev, 2008, 108: 3443–3480.

[30] H. Labiadh, K. Lahbib, S. Hidouri, S. Touil and T. B. Chaabane, Asian Pac. J. Trop. Med., 2016, 9, 757-762.

[31] D. A. Colantonio, C. Dunkinson, D. E. Bovenkamp and J. E. Van Eyk, Proteomics, 2005, 5, 3831-3835.
[32] H. Irving, S. Cooke, S. Woodger and R. Williams, J. Chem. Soc., 1949, 1847-1855.
[33] K. Sooklal, B. S. Cullum, S. M. Angel and C. J. Murphy, J.Phys. Chem., 1996, 100, 4551-4555.
[34] J. Tauc, Amorphous and liquid semiconductors, Springer Science & Business Media, 2012.
[35] J. P. Cornard, L. Dangleterre and C. Lapouge, J.Phys.Chem.A, 2005, 109, 10044-10051.
[36] Q. Zhao, X. Rong, H. Ma and G. Tao, J. Hazard. Mater., 2013, 250, 45-52.
[37] Z. Zhang, Y. Miao, L. Lian, and G. Yan, Anal. Biochem. 2015, 489, 17-24.
[38] S. C. Taiane, B. M. Tatiane, P. N. Keller, and N. Jaqueline, Food Sci. Human Wellness, 2018, **7**, 215–219.
[39] N. Pejic, V. Kuntic, Z. Vujic and S. Micic, Farmaco, 2004, 59, 21-24.
[40] H. Qiu, C. Luo, M. Sun, F. Lu, L. Fan and X. Li, Food Chem., 2012, 134, 469-473.
[41] P. Zuo, D. Xiao, M. Gao, J. Peng, R. Pan, Y. Xia and H. He, Microchim. Acta, 2014, 181, 1309-1316.

TABLE 1: Effect of foreign substance on the determination of quercetin.Concentrations: pH= 2.6, phosphate buffer 0.1 M,$C_{ZnS@Dz\ QDs}$= 39 μg mL^{-1}, $C_{Pb^{2+}}$ =140 μM,$C_{Que.}$= 1.0 μM

Interferance	**Tolerance limit (mol/mol)**
Al^{3+} , Fe^{3+}	1000
Ca^{2+}, Mg^{2+}, Zn^{2+}, Mn^{2+}, Cu^{2+}	1000
NH_4^+, K^+	1000
SO_4^{2-}, I^-, CN^-	1000
Valine, Gluconic acid, Methionine, Isoleucine, Cysteine, Urea, Arginine	1000
Na^+, Cl^-	500
Uric acid, Glucose, Ascorbic acid	500

TABLE 2: Recovery of the spiked quercetin in human serum and 24-h urine samples (Conditions: pH 2.6, phosphate buffer 0.1 M, $C_{ZnS@Dz\ QDs}$=39 μg. mL^{-1}, $C_{Pb^{2+}}$ =140 μM).

Serum sample	Added (μM)	Found by this method	RSD (n=3)	Recovery (%)	Urine sample	Added (μM)	Founded by this method	RSD (n=3)	Recovery (%)
S1	0	0.26	3.2	-	U1	0	0.25	9.9	-
	1.18	1.35 ± 0.02	1.2	92.3		1.18	1.27 ± 0.16	12. 8	92.8
	2.36	2.58 ± 0.02	1.0	98.2		2.36	2.66 ± 0.23	8.6	102.2
	3.55	3.92 ± 0.15	3.9	103.1		3.55	3.81 ± 0.28	7.3	100.6
	4.73	4.51 ± 0.04	0.9	91.8		4.73	4.47 ± 0.50	11.3	91.3
S2	0	0.11	7.9	-	U2	0	0.17	3.9	-
	1.18	1.08 ± 0.08	7.2	92.8		1.18	1.25 ± 0.01	7.9	91.4
	2.36	2.47 ± 0.10	3.9	99.8		2.36	2.64 ± 0.25	9.5	104.4
	3.55	3.23 ± 0.03	1.0	91.0		3.55	3.84 ± 0.33	8.6	103.5
	4.73	4.32 ± 0.05	1.1	94.0		4.73	4.63 ± 0.42	9.0	94.3
S3	0	0.049	12.1	-	U3	0	0.27	4.5	-
	1.18	1.10 ± 0.06	5.5	93.2		1.18	1.36 ± 0.18	13.2	91.7
	2.36	2.39 ± 0.01	0.3	98.9		2.36	2.58 ± 0.13	4.9	97.5
	3.55	3.48 ± 0.01	2.9	96.7		3.55	3.82 ± 0.06	1.5	99.9
	4.73	4.45 ± 0.11	2.6	93.0		4.73	4.47 ± 0.19	4.3	92.8
S4	0	0.049	10.2		U4	0	0.29	5.5	-
	1.18	1.10 ± 0.29	26.2	92.3		1.18	1.32 ± 0.14	10.7	93.4
	2.36	2.56 ± 0.18	7.0	106.1		2.36	2.62 ± 0.05	1.77	98.7
	3.55	3.65 ± 0.0.29	8.0	101.5		3.55	3.64 ± 0.43	11.9	94.4
	4.73	4.62 ± 0.66	14.3	96.7		4.73	4.40 ± 0.27	6.2	91.0
S5	0	0.22	2.8	-	U5	0	0.086	10.2	-
	1.18	1.18 ± 0.07	6.4	97.0		1.18	1.28 ± 0.17	13.2	100.8
	2.36	2.41 ± 0.19	7.8	100.8		2.36	2.42 ± 0.06	2.37	98.61
	3.55	3.70 ± 0.21	5.7	103.6		3.55	3.74 ± 0.20	5.26	103.0
	4.73	4.56 ± 0.35	0.8	95.9		4.73	4.72 ± 0.31	6.59	97.9
S6	0	0.077	3.2	-	U6	0	0.17	4.6	-
	1.18	1.26 ± 0.16	12.6	100.0		1.18	1.34 ± 0.09	6.73	99.0
	2.36	2.29 ± 0.09	3.9	93.5		2.36	2.54 ± 0.15	5.79	100.4

	3.55 4.73	3.57 ± 0.10 4.58 ± 0.30	3.0 6.6	98.3 95.1		3.55 4.73	3.90 ± 0.17 4.71± 0.23	4.27 4.97	105.4 96.2

[a] (Mean ± SD; n=3)

TABLE 3: Comparison of the analytical parameters of the developed probe with the other reported methods for the detection of quercetin

Methods	Used nanoparticles	Linear range (μM)	Detection limit (μM)	RSD (%)	Response time (min)	Real sample	Ref.
Raman spectroscopy	-	50.0-149.9	50.0	0.3	-	Dried onion peels	19
Fluorometry	MPA-ZnS QDs	2.6-7.5	0.6	1.56	10	Fetal bovine serum	23
Fluorometry	CdSe/ZnS	1.9-608.8	0.46	2.9	10	Synthetic samples	24
Phosphorimetry	MPA-capped Mn-doped ZnS QDs	0.33-19.85	0.16	4.6	15	Urine and serum	37
UV-Vis. Spectrophotometry	-	3.3-39.7	2.5	3	4	Pure and pharmaceutical dosage form	39
Flow injection chemiluminescence	-	1.4-159.8	0.93	2.7-3.3	-	Drug	40
Fluorometry	Carbon NPs	3.3-41.2	0.175	2.8	22	Fetal bovine serum	41
Fluorometry	DZ-capped ZnS QDs	0.5-21.7	0.25	2.1	Instantly	Urine and serum	This work

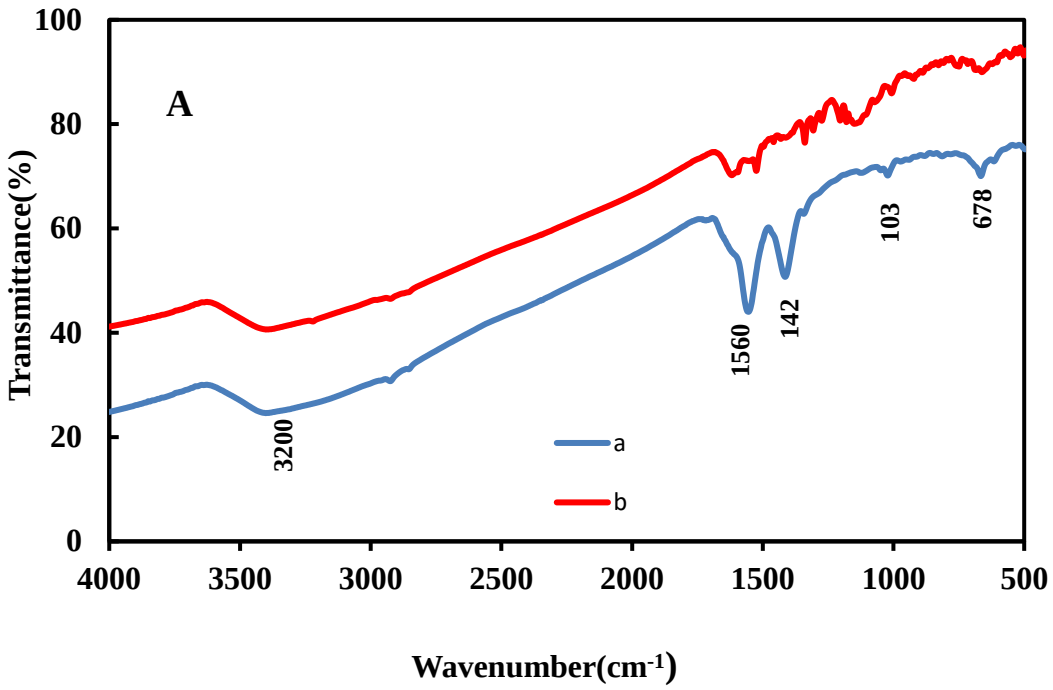

Fig. 1A

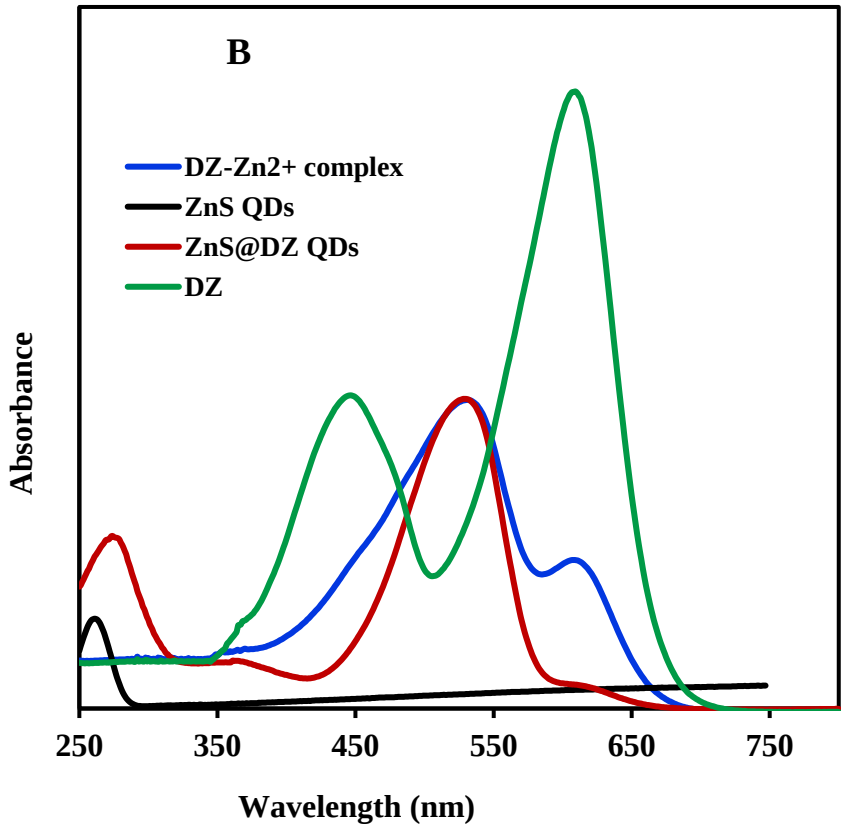

Fig. 1B

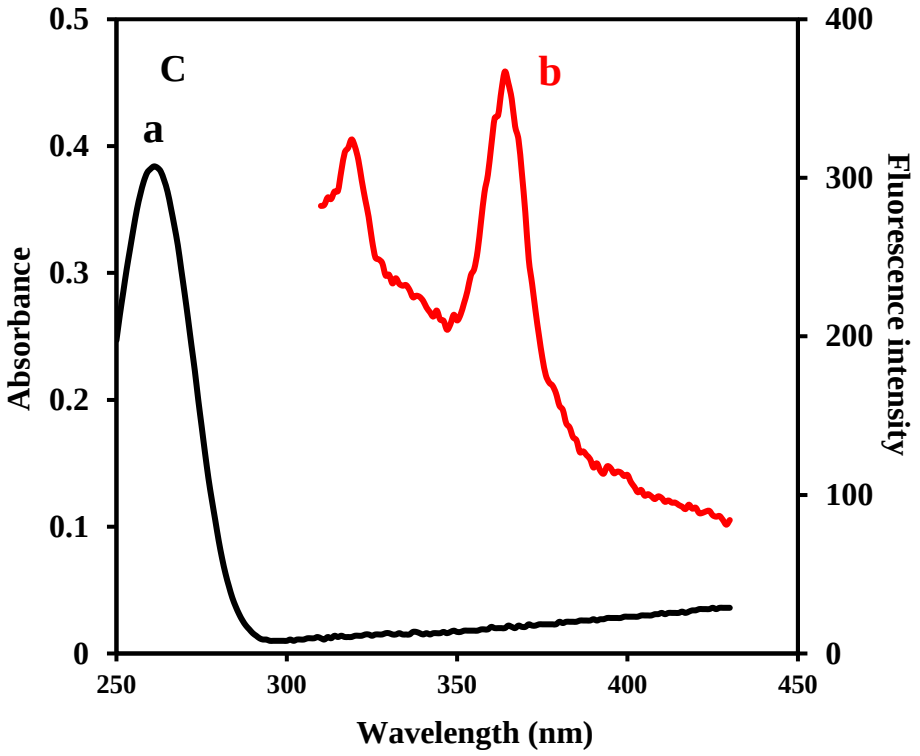

Fig. 1C

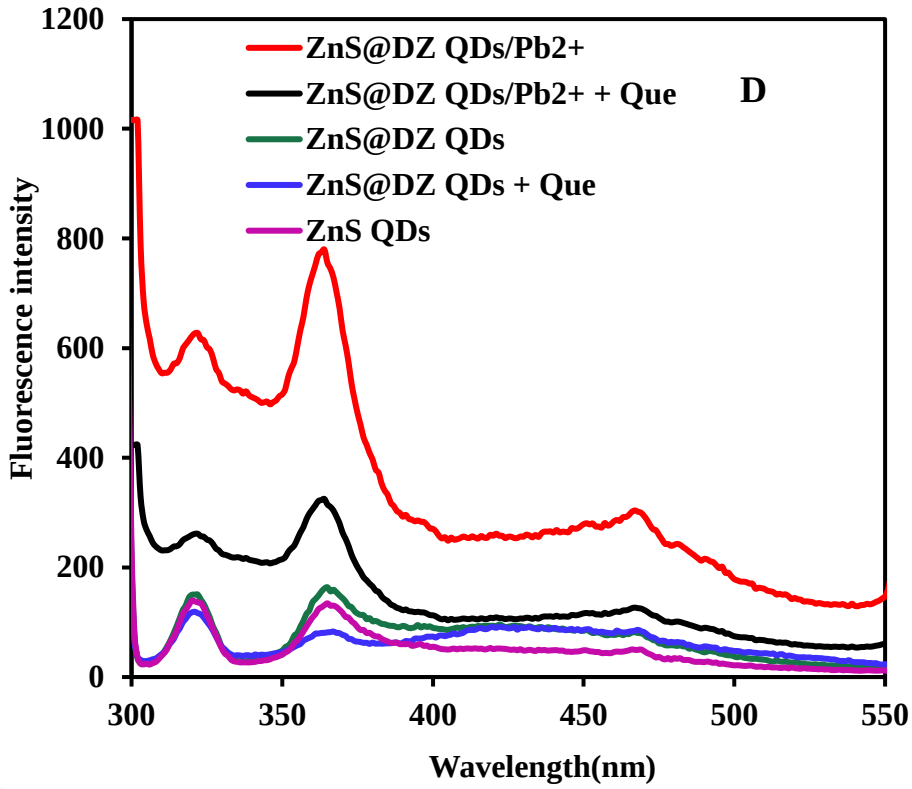

Fig. 1D

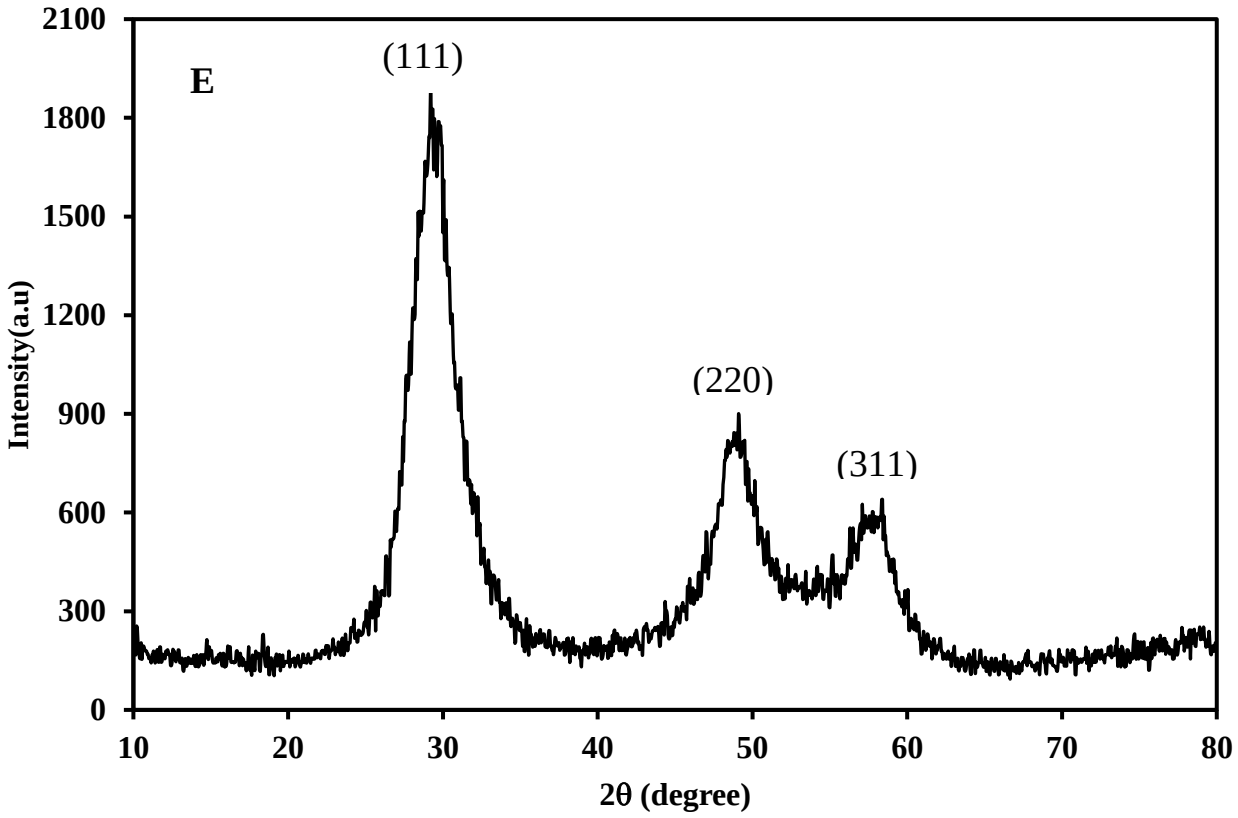

Fig. 1E

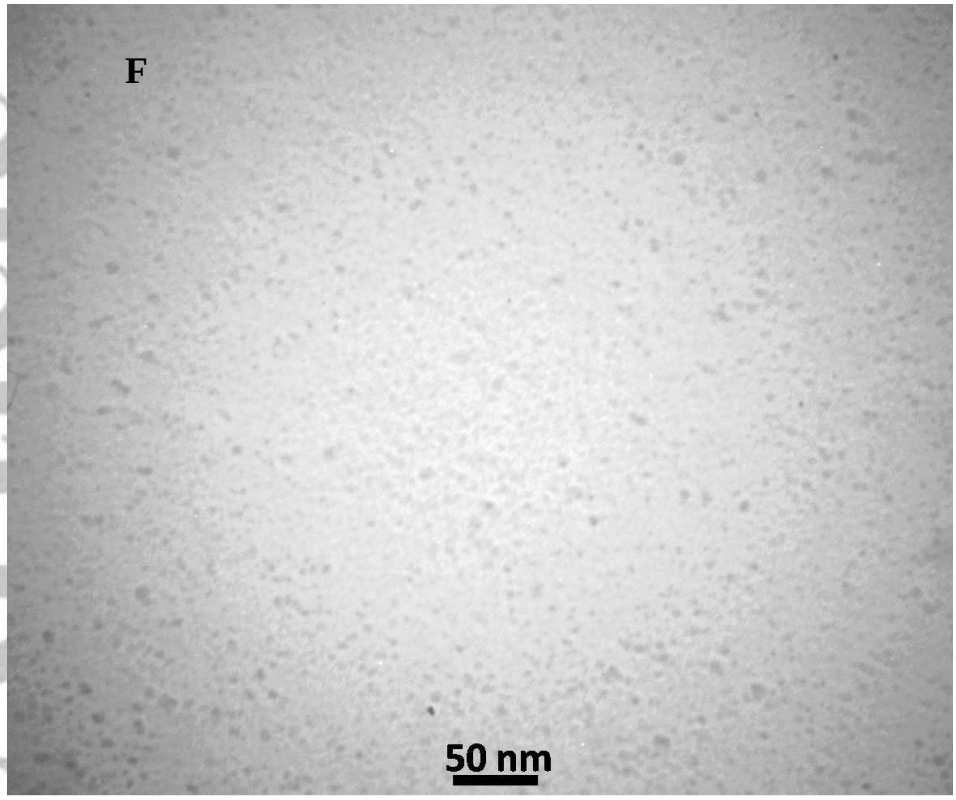

Fig. 1 F

FIGURE 1 (A): The FT-IR spectra of a) the ZnS QDs and b) the ZnS@DZ QDs; (B): UV–Vis absorption spectra of the ZnS QDs, ZnS@DZ QDs, DZ-Zn^{2+} complex, and DZ (C): (a)The UV-Vis absorption and (b) fluorescence emission spectra of ZnS@DZ QDs, (D): Fluorescence spectra of ZnS QDs, ZnS@DZ QDs, ZnS@DZ QDs with the addition of Pb^{2+}(ZnS@DZ QDs/Pb^{2+}), ZnS@DZ QDs with the addition of quercetin (Zn@DZ QDs + Que), Zn@DZ QDs with the addition of Pb^{2+} and quercetin (Zn@DZ QDs/Pb^{2+} + Que); (E): XRD pattern of ZnS@DZ QDs; (F) TEM image of ZnS QDs.

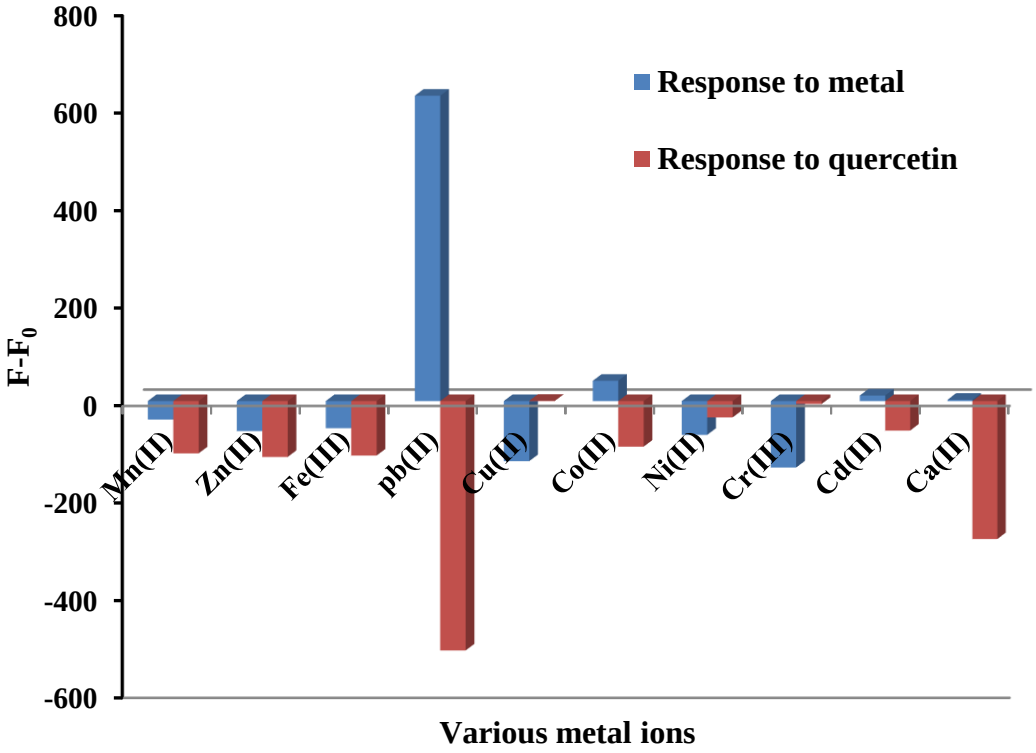

FIGURE 2 The response of ZnS@DZ in the presence of some metals as a probe for determination of quercetin.Conditions: pH 3, $C_{ZnS@Dz\ QDs}$= 32 µg mL^{-1}, $C_{metal\ ions}$= 100 µM, $C_{Que.}$ = 1.0 µM.

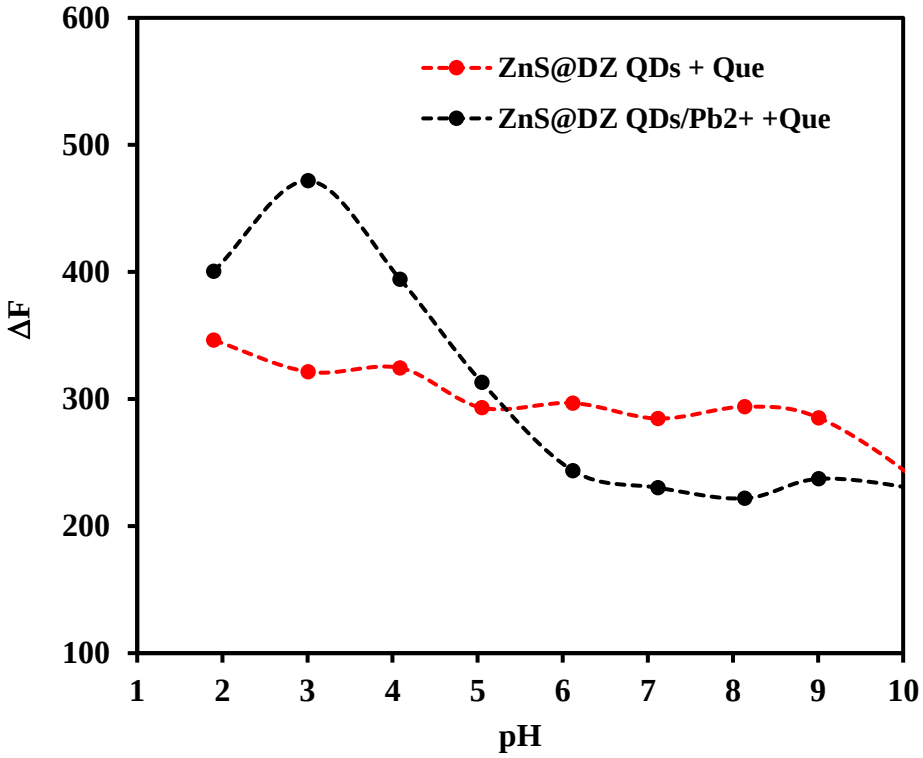

FIGURE 3 The effect of pH on the response of the ZnS@DZ QDs with and without Pb^{2+} for the determination of quercetin. Conditions: $C_{ZnS@Dz\ QDs}$ = 32 μg m L^{-1}, $C_{Pb^{2+}}$ = 100 μM, $C_{Que.}$ = 1.0 μM.

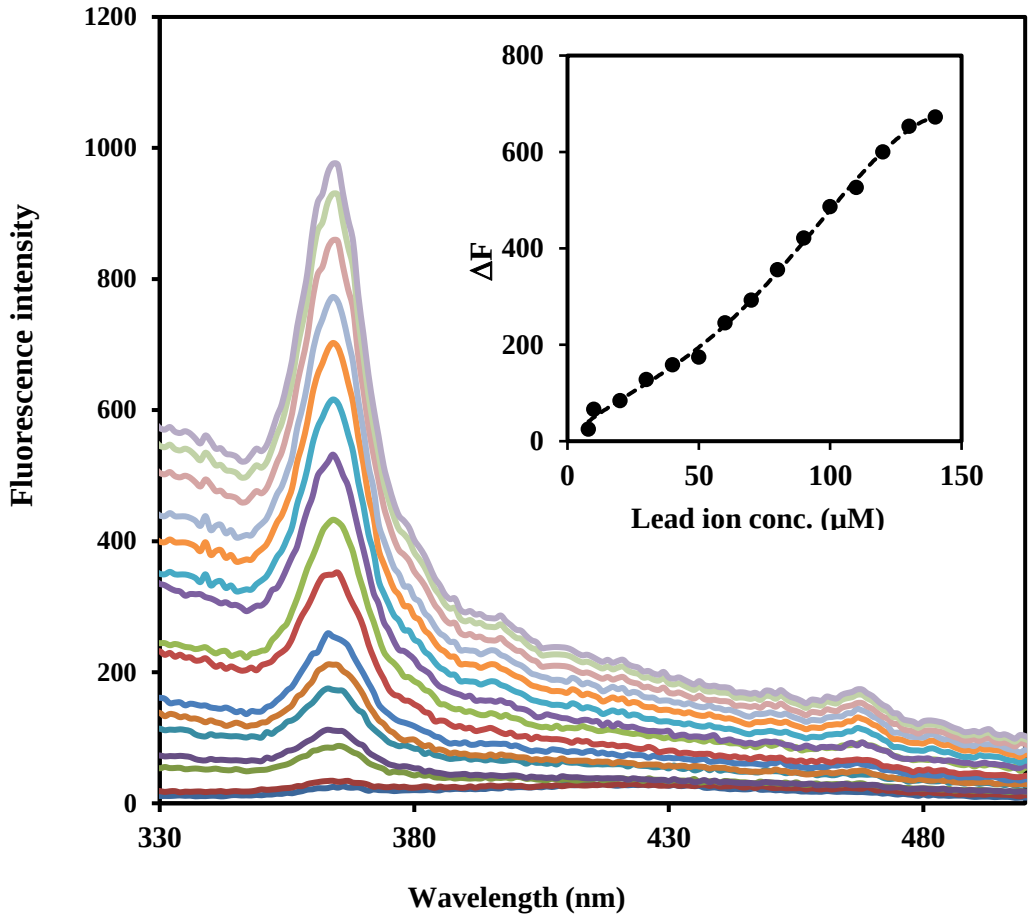

FIGURE 4 The ZnS@DZ emission in the presence of different concentration of Pb^{2+} (a) 8, (b) 10, (c) 20, (d) 30, (e) 40, (f) 50, (g) 60, (h) 70, (i) 80, (j) 90, (k) 100, (l) 110, (m) 120, (n) 130, and (o) 140 µM for determination of quercetine. Inset displays the plot of ΔF response against Pb^{2+} concentrations. Conditions: pH 2.6, phosphate buffer 0.1 M, $C_{ZnS@Dz\ QDs}$ = 32 µg mL^{-1}, C_{Que}=1.0 µM.

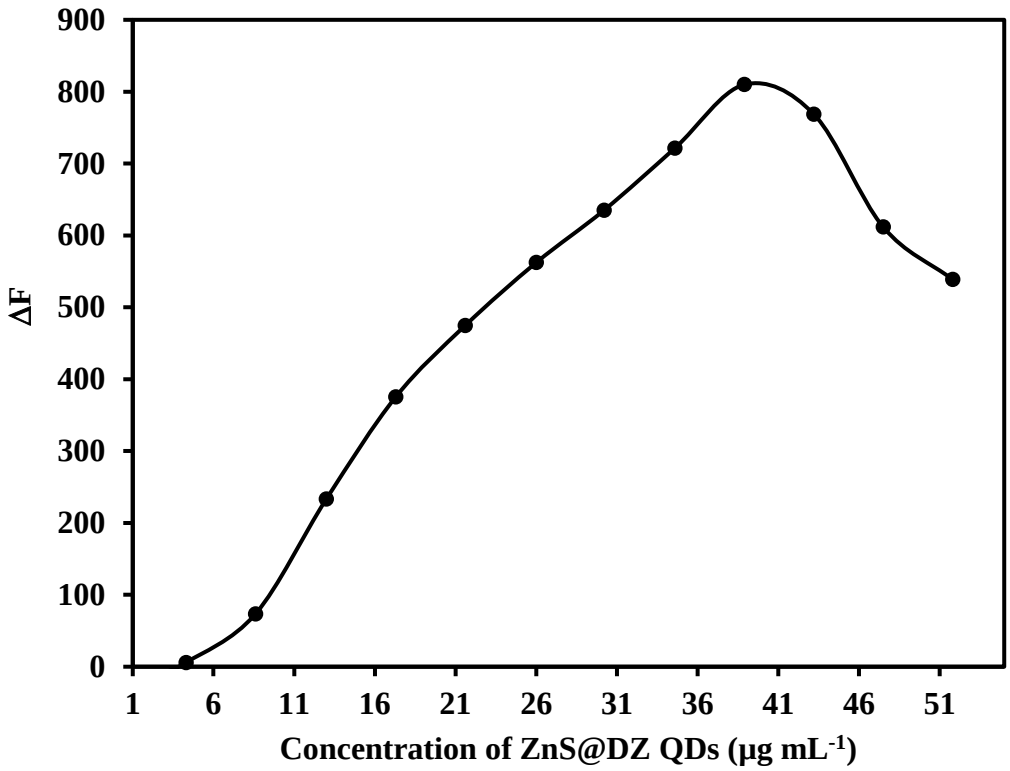

FIGURE 5 Effect of ZnS@DZ QDs concentration on the fluorescence intensity of the probe. Conditions: pH 2.6, phosphate buffer 0.1 M, $C_{Pb^{2+}}$ = 140 μM, $C_{Que.}$= 1.0 μM.

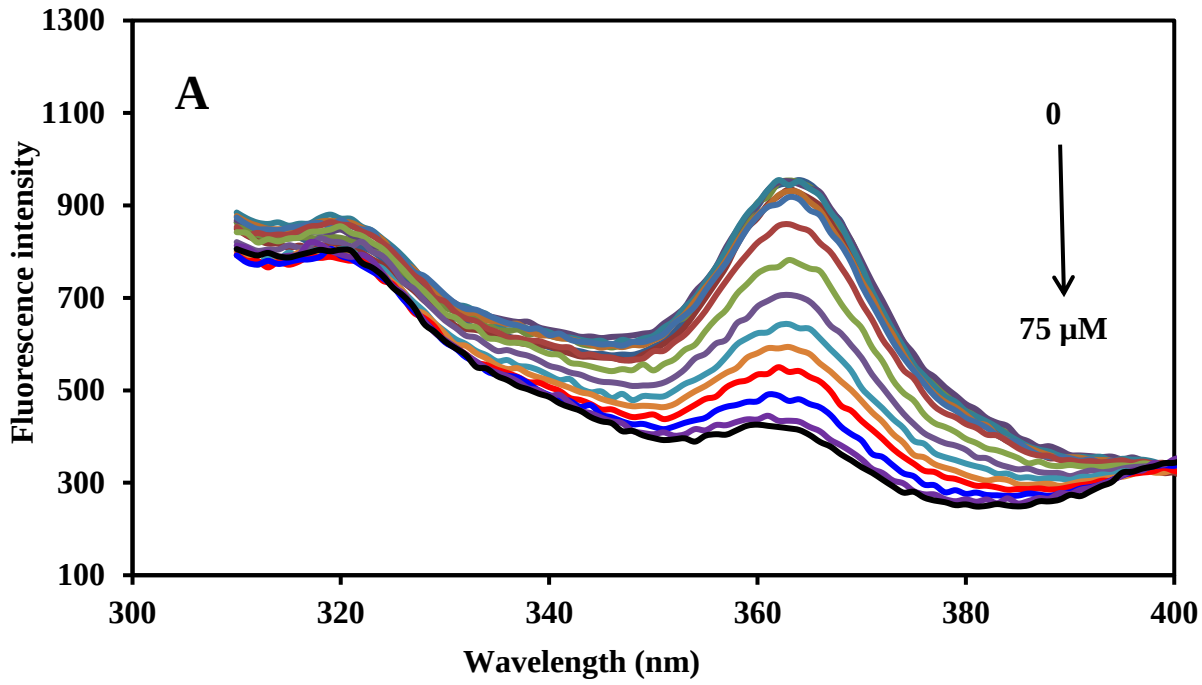

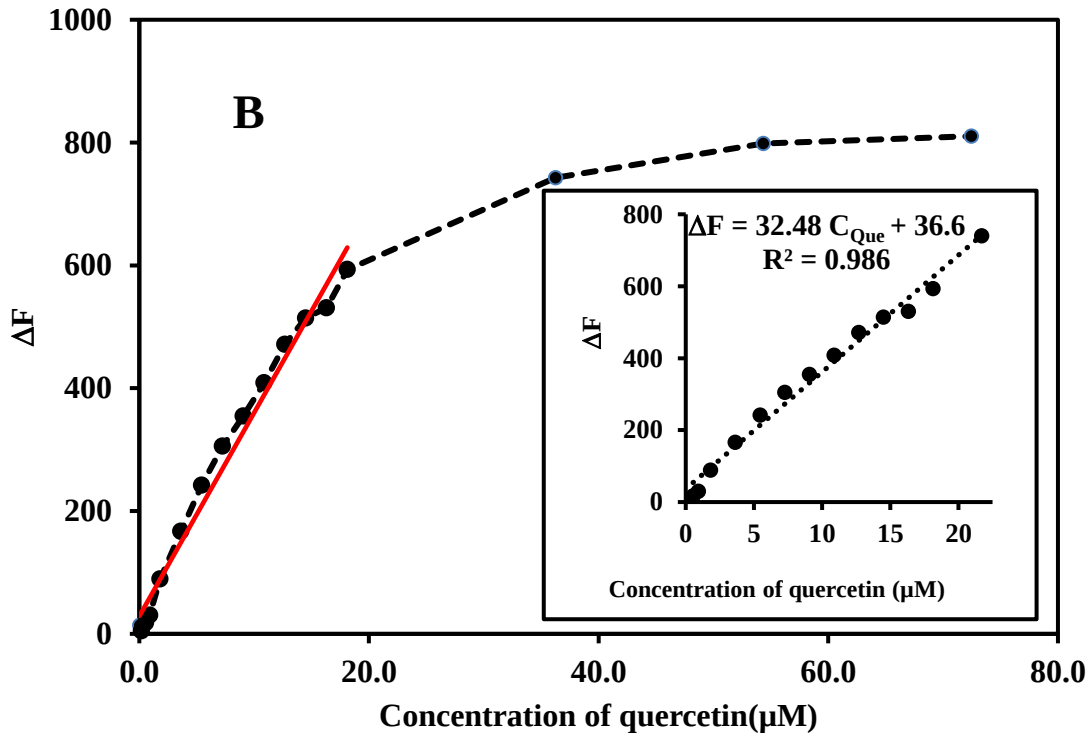

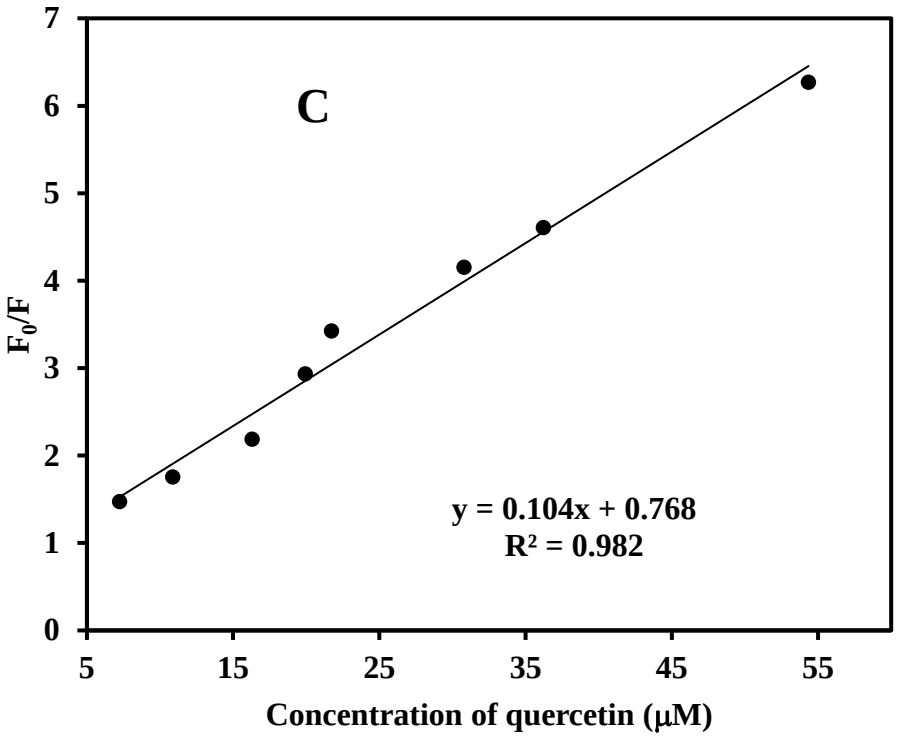

FIGURE 6 Fluorescence emission spectra of ZnS@DZ QDs/Pb^{2+} probe after the addition of different concentrations of quercetin, (B) the ΔF response of the probe aginst quercetin concentrations.The inset shows the linear calibration plot of the probe toward quercetin; Conditions: pH 2.6, phosphate buffer 0.1 M,$C_{ZnS@Dz\ QDs}$= 39.0 μg mL^{-1}, $C_{Pb^{2+}}$= 140 μM

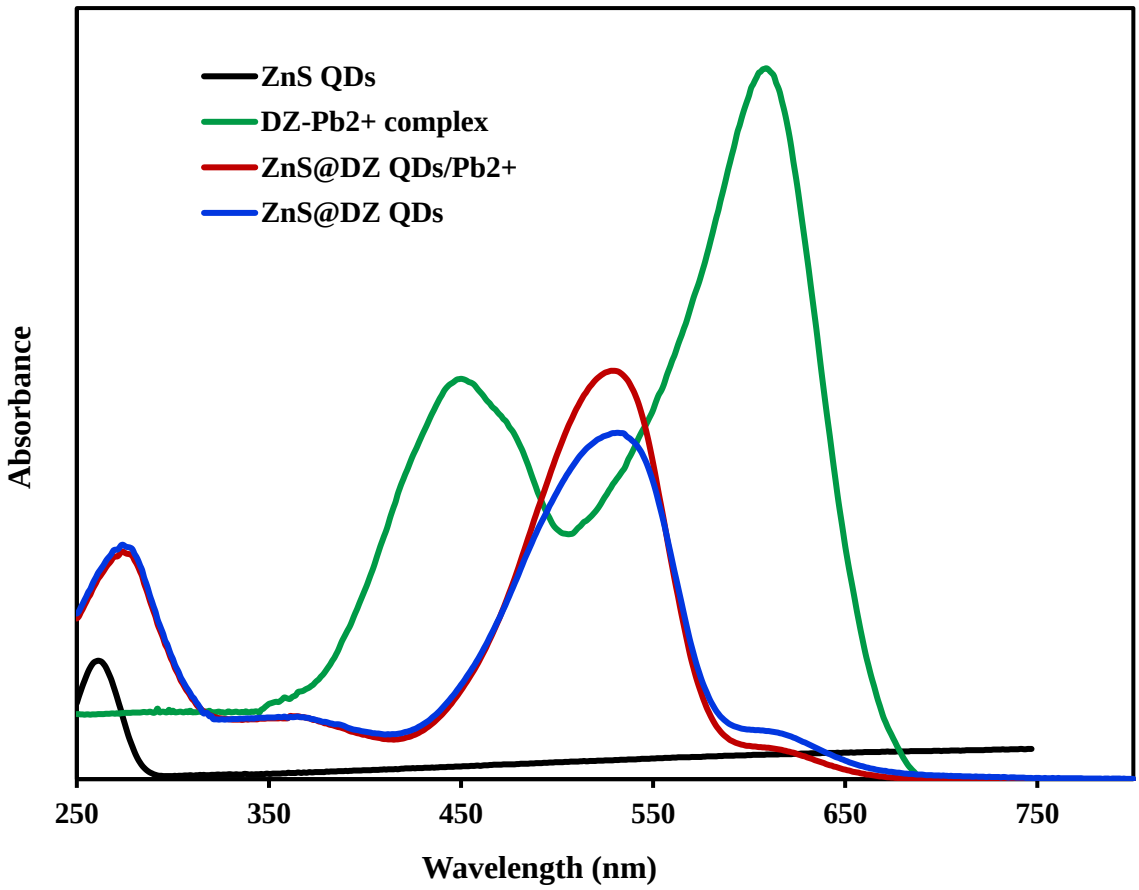

FIGURE 7. UV-Vis. Absorption spectra of ZnS QDs, ZnS@DZ QDs, DZ-Pb^{2+} complex, and ZnS@DZ QDs/Pb^{2+}.

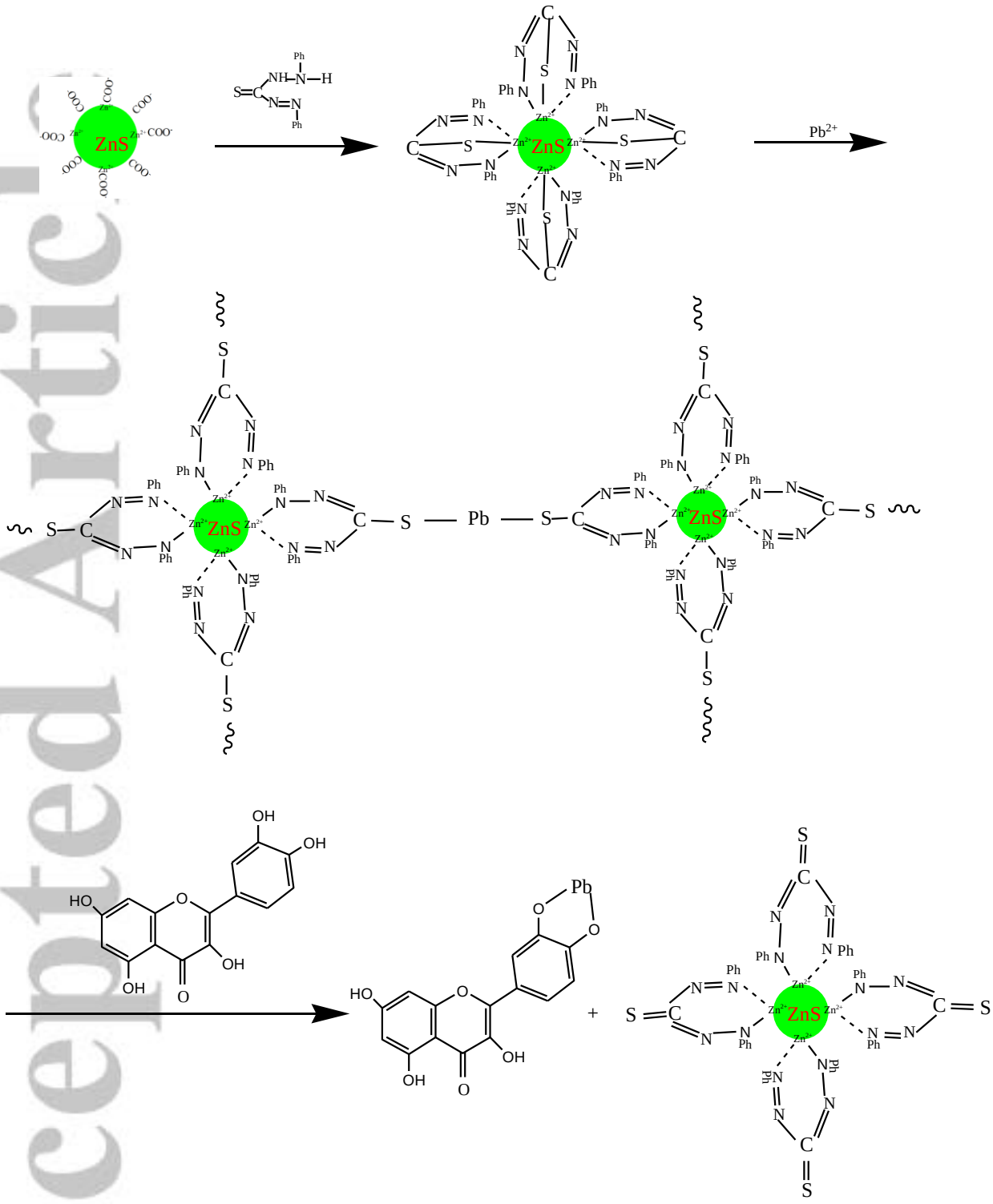

SCHEME 1. Schematic illustration of the proposed mechanism for detection of quercetin by ZnS@DZ/Pb^{2+} probe

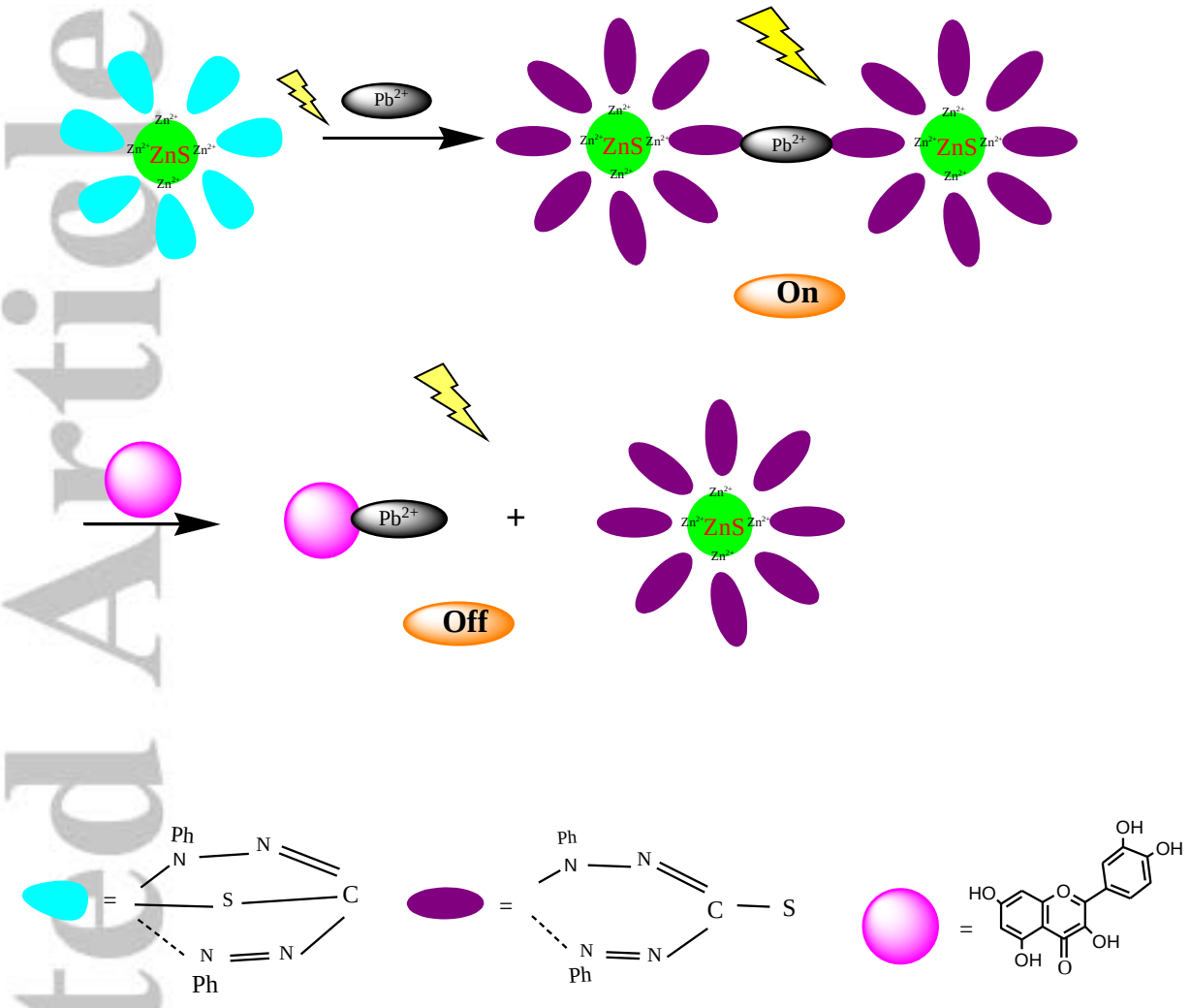

A turn on/turn off ZnS QDs capped with dithizone (ZnS@DZ QDs) probe to high selectivite and fast response toward quercetin.